Received: 29 June 2023 | Revised: 9 September 2023 | Accepted: 3 October 2023

DOI: 10.1002/app.54828

RESEARCH ARTICLE

Applied Polymer SCIENCE WILEY

Composites produced from waste plastic with agricultural and energy sector by-products

Claudia V. Lopez | **Rhett C. Smith**

Department of Chemistry and Center for Optical Materials Science and Engineering Technology, Clemson University, Clemson, South Carolina, USA

Correspondence
Rhett C. Smith, Department of Chemistry and Center for Optical Materials Science and Engineering Technology, Clemson University, Clemson, SC 29634, USA.
Email: rhett@clemson.edu

Funding information
National Science Foundation, Grant/Award Number: 2203669

Abstract

A three-stage route to chemically upcycle post-consumer poly(ethylene terephthalate) (PET) to produce high compressive strength composites is reported. This procedure involves initial glycolysis with diethylene glycol to produce a mixture (GPET) comprising oligomers of 2–7 terephthalate units followed by trans/esterification of GPET with fatty acid chains supplied by brown grease, an agricultural by-product of animal fat of relatively low nutritional or fuel value. This process yields PGB comprising a mixture of mono-terephthalate ester derivatives. The olefin units provided by unsaturated fatty acid chains in brown grease were crosslinked by an inverse vulcanization reaction with elemental sulfur to give composites GBS_x (x = wt% S, varied from 80%–90%). The compressive strengths of GBS_{80} (27.5 ± 2.6 MPa) and GBS_{90} (19.2 ± 0.8 MPa) exceed the compressive strength required of ordinary Portland cement (17 MPa) for its use in residential building foundations. The current route represents a way to repurpose waste plastic, energy sector by-product sulfur, and agricultural by-product brown grease to give high strength composites with mechanical properties suggesting their possible use to replace less sustainably sourced legacy structural materials.

KEYWORDS

brown grease, inverse vulcanization, sulfur, sustainable composites, triglyceride

1 | INTRODUCTION

Structural materials are central to modern civilization, yet their production is a threat to our long-term well-being. For example, many widely used plastics are currently made from petrochemically derived olefins, and Portland cement production releases ~8% of anthropogenic CO_2.[1] More sustainable alternatives are urgently needed. Replacing petrochemical olefins with plant-derived unsaturated units and exploring alternative structural and packaging materials derived from such olefins has been extensively explored as part of a transition to a greener and more sustainable future economy. Unsaturated triglycerides are the primary constituents of plant oils, so these, along with terpenoids, are the most well-studied bio-derived olefins.[2–5] A much less well-explored area of research is the use of animal-derived fats as precursors to plastics and other structural materials. Sustainability scientists have suggested a proportionally higher net carbon footprint of animal- versus plant-derived food production,[6] despite the much higher percentage of animal products converted to commercial products versus

the large quantity of biomass waste produced by plant-based agriculture.[7] This larger relative carbon footprint makes elucidating additional carbon-negative/carbon-sequestering utility for animal coproducts an essential pursuit.

Some efforts have been made to produce biodiesel from less nutritionally valuable animal products such as trap grease, dissolved air flotation solids, and brown grease, but plant oils remain the most common precursors for biodiesel production on an industrial scale.[8,9] Among animal fats, brown grease is an especially attractive candidate for use as a chemical feedstock because it is a nutritionally less-valuable and high-volume coproduct of animal fat rendering.[7,10–12] Brown grease is essentially partially rancidified/hydrolyzed animal fat and is subject to regulations limiting its use in human or animal feed or as fertilizer, so it is an agricultural by-product of lower economic value. Chemically, brown grease is composed largely of free fatty acids and triglycerides. The olefin units in unsaturated fatty acid chains in triglycerides or fatty acid chains can be readily crosslinked by their vulcanization (or inverse vulcanization) with energy sector by-product sulfur.[13–15] This reactivity of unsaturated units in brown grease inspired a recent report in which brown grease was used as a component of carbon-sequestering cements as an example of the potential for animal fat use to replace petrochemical olefins in the synthesis of structural materials.[16]

The formation of polymers and composites from olefin-bearing substrates such as brown grease with majority component elemental sulfur occurs by the process of inverse vulcanization,[17] an atom-economical process whereby thermally generated S-centered radicals form C_{alkyl}—S bonds with olefins to yield cross-linked networks (Scheme 1). Although the precise mechanism of this process is still under investigation,[18] its applicability to a wide range of substrates has been demonstrated,[13,19–33] and significant progress has been made to lower the energy requirements and improve processability of the resulting high sulfur content materials (HSMs).[24,25,34–39]

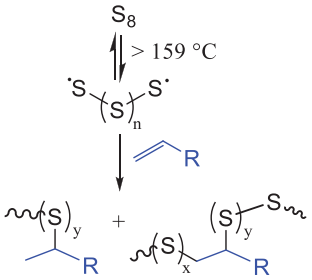

SCHEME 1 General inverse vulcanization of an olefin with sulfur. [Color figure can be viewed at wileyonlinelibrary.com]

HSMs prepared by these C—S bond-forming processes have found promise for a panoply of diverse applications including transparent lenses for thermal imaging,[40] absorbents,[41–45] electrode materials,[46–55] and fertilizers.[56,57] We recently reported additional uses of elemental sulfur in processes to recycle/upcycle waste plastic.[58–60] One of these applications involved the chemical recycling of poly(ethylene terephthalate) (PET) via sequential glycolysis, esterification with oleoyl chloride, and inverse vulcanization with elemental sulfur (Scheme 2). This process resulted in mPES, a HSM having compressive strength of 26.9 ± 0.6 MPa and flexural strength/moduli of 7.7/320 MPa. Impressively, these metrics exceed those of some Portland cements used in building foundations (compressive strengths of ≥17 MPa and flexural strengths of ~3.5 MPa are required). Although this was an important proof-of-principle study to demonstrate the formation of high compressive strength composites from fatty acid-derivatized PET oligomers, the use of expensive oleoyl chloride as the unsaturated chain source precludes direct commercial application of this process for industrial recycling/upcycling of PET. If oleoyl chloride could be replaced with an alternative fatty acid chain source such as waste product brown grease to

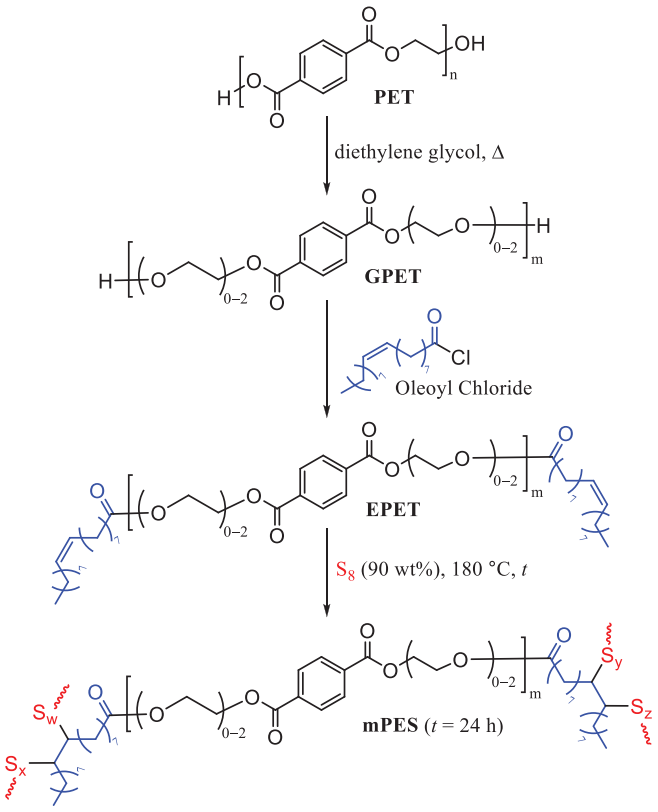

SCHEME 2 Sequential glycolysis, esterification, and vulcanization of poly(ethylene terephthalate). [Color figure can be viewed at wileyonlinelibrary.com]

yield composites having properties similar to those achieved in mPES, the economic viability of this route would be significantly improved. In the current context, it was of interest to (1) assess the potential trans/esterification reaction between the glycolyzed-PET (GPET) and brown grease to incorporate olefinic units; (2) assess the extent to which olefins of the glycolyzed-PET/brown grease reaction product can undergo inverse vulcanization with elemental sulfur; and (3) analyze the thermal and mechanical properties of resulting HSMs.

Herein, we report the transformation of post-consumer PET by glycolysis to give GPET[60] followed by trans/esterification with brown grease to give PGB, and finally reaction of 10–20 wt% PGB with elemental sulfur to yield composites GBS_x (x = wt% S, varied from 80% to 90%). The chemical, thermal, and mechanical properties of these composites are detailed.

2 | EXPERIMENTAL PROCEDURES

2.1 | General considerations

All NMR spectra were recorded on a Bruker (USA) Avance spectrometer operating at 300 MHz for proton nuclei on samples dissolved in $CDCl_3$ and referenced to tetramethylsilane (with a proton resonance set to 0.00 ppm).

Fourier transform infrared (FTIR)spectra were obtained using a Shimadzu (Japan) IRAffinity-1S with an attenuated total reflectance (ATR) attachment. Scans were collected over the range 400–4000 cm^{-1} at ambient temperature with a resolution of 8 cm^{-1}.

Thermogravimetric analysis (TGA) was recorded on a Mettler Toledo (Switzerland; TGA 2 STARe System) over the range 20–800°C with a heating rate of 10°C min^{-1} under a flow of N_2 (100 mL min^{-1}). Each measurement was acquired in duplicate and presented results represent an average value. Differential scanning calorimetry (DSC) was acquired (Mettler Toledo DSC 3 STARe System) over the range −60 to 140°C with a heating rate of 10°C min^{-1} under a flow of N_2 (200 mL min^{-1}). Each DSC measurement was carried out over three heat/cool cycles.

Scanning electron microscope (SEM) was acquired on a Schottky Field Emission Scanning Electron Microscope SU5000 (Hitachi, Japan) operating in variable pressure mode with an accelerating voltage of 15 keV.

Matrix-assisted laser desorption/ionization time of flight mass spectrometry (MALDI-TOF) spectra were recorded on a MicrofleX LRF spectrometer (Bruker, USA) equipped with a 337-nm nitrogen laser in the positive reflectron ion mode. The scanning mass-to-charge (m z^{-1}) range for the experiments was between 600 and 1600 using α-cyano-4-hydroxycinnamic acid as the matrix.

Compressional analysis was performed on a Mark-10 ES30 test stand (USA) equipped with a M3-200 force gauge (1 kN maximum force with ±1 N resolution) with an applied force rate of 3–4 N s^{-1} in a modification of ASTM C39 test protocol. Compression cylinders were cast from silicone resin molds (Smooth-On Oomoo® 30 tin-cure) with diameters of approximately 6 mm and heights of approximately 10 mm. Samples were manually sanded to ensure uniform dimensions and measured with a digital caliper with ±0.01-mm resolution. Compressional analysis was performed in triplicate and results were averaged.

Flexural strength analysis was performed using a Mettler Toledo (Switzerland) DMA 1 STARe System in single cantilever mode in modification of ASTM D790. Flexural strength samples were cast from silicone resin molds (Smooth-On Oomoo® 30 tin-cure). The sample dimensions were 1.5 × 10.4 × 5.0 mm. The clamping force was 1 cN m and the temperature was 25°C. The samples were tested in duplicates and the results were averaged.

For percent crystallinity calculations, ΔH_m and ΔH_{cc}, the data were taken from the third heat/cool cycles. Melting enthalpies and the cold crystallization enthalpies were calculated using DSC data. The percent crystallinity of the composites GBS_{90} and GBS_{80} with respect to sulfur was calculated using the following equation:

$$\Delta\chi_c = \left\{\frac{\Delta H_{m(GBSx)} - \Delta H_{cc(GBS)}}{\Delta H_{m(S)}}\right\} * 100\%,$$

where $\Delta\chi_c$ is the change in percentage crystallinity with respect to sulfur, $\Delta H_{m(GBS)}$ is the melting enthalpy of composite materials (GBS_x), $\Delta H_{cc(GBS)}$ is the cold crystallization enthalpy of composite materials (GBS_x), $\Delta H_{m(S)}$ is the melting enthalpy of sulfur, and $\Delta H_{cc(S)}$ is the cold crystallization enthalpy of sulfur.

Carbon disulfide (CS_2) extractions were performed by suspending 0.3 g of finely ground material in 20 mL of CS_2, allowing the solid to settle for 30 min, pipetting off the supernatant into a separate vial, and adding another 20 mL of CS_2. This process was repeated an additional three times so that a total of five washes were performed. The residual CS_2 was evaporated under a flow of N_2, and each vial was weighed to determine the fraction that was soluble (collected as supernatant) or insoluble (remained in the initial vial).

2.2 | Materials and methods

Brown grease (supplied by the Animal Coproducts Research and Education Center) and zinc acetate (Sigma-Aldrich) were used as received. PET was obtained directly from post-consumer water bottles and prepared for reaction as previously reported.[59] The composite materials were allowed to stand at room temperature for 4 days prior to analysis. A sample of the same batch of GPET used in our previous report[60] was also used in the current study.

CAUTION: Heating elemental sulfur with organics can result in the formation of H_2S gas. H_2S is toxic, foul smelling, and corrosive. Although we did not observe any mass loss attributable to gas generation, temperature must be carefully controlled to prevent thermal spikes, which contribute to the potential for H_2S evolution. Rapid stirring and very slow addition of reagents can help prevent unforeseen temperature spikes.

2.3 | Synthesis of PGB

The preparation of PGB involved the reaction of GPET (2.10 g) with brown grease (5.09 g) and zinc acetate (1.00 g, 5.54 mmol). The reaction mixture was stirred for 24 h at 185°C in a round-bottom flask equipped with a reflux condenser under a flow of dry nitrogen gas. The final material was a brown, slightly viscous, and homogeneous liquid product that was used without further purification.

2.4 | Synthesis of GBS_{90}

Preparation of GBS_{90} involved the reaction of PGB (2.12 g, 10 wt%) and sulfur (18.11 g, 90 wt%). Sulfur was first melted in an oil bath at 160°C with rapid mechanical stirring. Then, the temperature was raised further to 185°C. Once the temperature was stable, PGB was slowly added to the sulfur while stirring. The reaction mixture was stirred for 24 h at 180°C, over which time a homogeneous solution was produced. Upon cooling to room temperature, the material solidified to a black solid composite in quantitative yield. ELEM. ANAL calc'd: C 6.00, H 1.00, S 90.00; found: C 4.90, H 0.20, S 94.06.

2.5 | Synthesis of GBS_{80}

Preparation of GBS_{80} involved the reaction of PGB (4.22 g, 20 wt%) and sulfur (16.23 g, 80 wt%). Sulfur was first melted in an oil bath at 160°C with rapid mechanical stirring. Then, the temperature was raised to 185°C. Once the temperature was stable, PGB was slowly added to the sulfur while stirring. The reaction mixture was stirred for 24 h at 180°C, over which time a homogeneous solution was produced. Upon cooling to room temperature, the material solidified to a black solid composite in quantitative yield. ELEM. ANAL calc'd: C 10.00, H 1.00, S 80.00; found: C 15.22, H 1.05, S 79.50.

3 | RESULTS AND DISCUSSION

3.1 | Depolymerization and transesterification

Post-consumer PET bottles ($M_n = 44{,}000$, $M_w = 82{,}000$, PDI = 1.9) were processed and converted to GPET via glycolysis with diethylene glycol as previously reported.[60] GPET is a mixture comprising oligomers of 2–7 terephthalate units each and having ethylene glycol- or diethylene glycol-derived end groups. The next step in the process was the trans/esterification of GPET with brown grease. Brown grease used in the trans/esterification of GPET was from the same sample used to prepare mPES in a previous study,[16] a sample that was 34.18% free fatty acids, 0.57% moisture content, 0.81% of unidentified impurities and the balance was acyl glycerides, with a total brown grease olefin content of 3.24 mmol g^{-1}.

It was hypothesized that the ester linkages in GPET would undergo transesterification with acyl glycerides/fatty acids in the brown grease and that the glycol end groups would likewise be esterified, giving a mixture of trans/esterification products in which vulcanization-capable unsaturated units have been covalently linked to PET-derived fragments (Scheme 3). GPET was therefore reacted with brown grease in a ~2:5 mass ratio under an atmosphere of N_2 for 24 h at 185°C to yield the esterified product mixture PGB (Scheme 3). PGB was identified to be the expected mixture of esterified terephthalate derivatives on the basis of its analysis by FT-IR spectroscopy, MALDI-TOF spectrometry, and ^1H NMR spectrometry. Thermal stability properties were assessed by TGA.

The FT-IR spectrum of PGB (Figure 1) provided initial evidence for successful trans/esterification of GPET. The infrared spectra for starting material GPET show the ester carbonyl (C═O) stretch at 1713 cm^{-1}, a broad O—H stretch at about 3400 cm^{-1}, and C—O stretches of the ester groups at 1100–1300 cm^{-1} (Figure S1). In contrast, the infrared spectra for the PGB product (Figure S2) showed the complete disappearance of the O—H stretch band, indicating consumption of glycol end groups, and a shift in the ester carbonyl stretch from 1713 to 1728 cm^{-1}

accompanied by significantly increased relative intensity of sp^3-C—H stretches (2800–2930 cm^{-1}), appearance of C—O stretches (1100–1300 cm^{-1}) attributable to newly installed brown grease-derived ester groups, and the emergence of the ═C—H stretch (2950 cm^{-1}) and a weak C═C stretch band at around 1650 cm^{-1}.

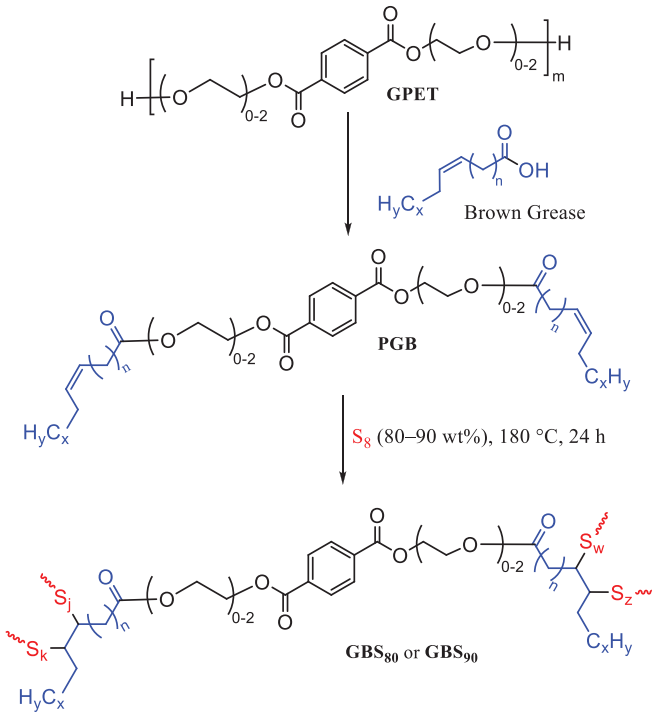

SCHEME 3 Trans/esterification of GPET with brown grease followed by the vulcanization of PET to yield GBS_x composites. GPET, glycolyzed-poly(ethylene terephthalate); PET, poly(ethylene terephthalate). [Color figure can be viewed at wileyonlinelibrary.com]

The molecular weights of oligomers present in PGB were elucidated by MALDI-TOF spectrometry, which further confirmed the esterification reaction of the terminal alcohol moieties in GPET with the fatty acid chains present in brown grease (Figure 2; proposed structures are provided in Table S1). Baseline resolution of individual species differing only in degree of unsaturation was not achieved in the MALDI-TOF spectrum due to their similar molecular weights—species within one degree of unsaturation have a molecular weight difference of only 2 g mol^{-1} for a —CH_2CH_2— versus a —CH═CH— unit in a molecule comprising up to 58 carbon atoms. The extent to which unsaturated units suitable for inverse vulcanization had been incorporated thus could not be determined from the MALDI data, and ^{1}H NMR spectrometry was employed for this purpose.

Proton NMR spectrometry of PGB with 2,3,4,5,6-pentafluorobenzaldehyde added as an internal standard was used to quantify the total olefin content of PGB (inset in Figure 3, full spectrum in Figure S1). In this analysis, a calculation based on the ratio of integration for PGB olefinic proton resonances (~5.5 ppm) versus that for the aldehydic proton resonance (~10.4 ppm) of the known quantity of internal standard revealed that the olefin content of PGB was 1.13 mmol g^{-1}.

Thermogravimetric analysis of PGB (Table 1 and Figure 4) showed a decomposition temperature (T_d, here defined as the temperature at which 5% mass loss is observed to occur upon heating under N_2) of 224°C. The thermal decomposition of PGB predictable shows a first decomposition step between 185–310°C attributed to decomposition of ester functionalities and a second decomposition step at 400–450°C attributable to decomposition of aromatic-rich PET oligomer-derived moieties

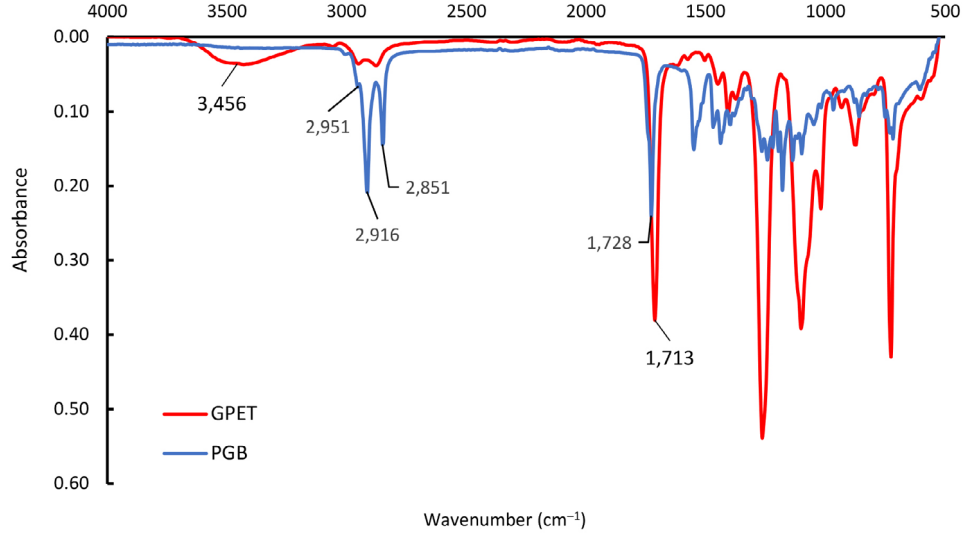

FIGURE 1 Fourier-transform infrared spectroscopy traces for glycolyzed-poly(ethylene terephthalate) (GPET) and PGB. [Color figure can be viewed at wileyonlinelibrary.com]

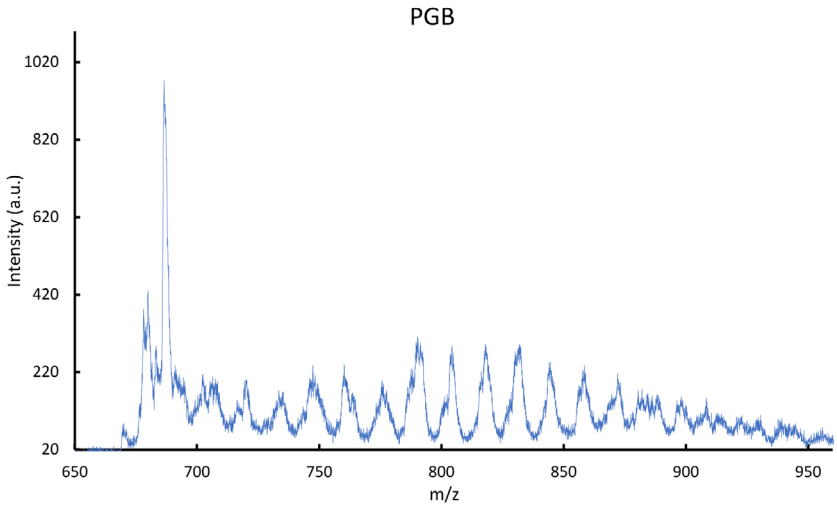

FIGURE 2 Matrix-assisted laser desorption/ionization time-of-flight mass spectrometry spectra in the positive reflectron ion mode for PGB. [Color figure can be viewed at wileyonlinelibrary.com]

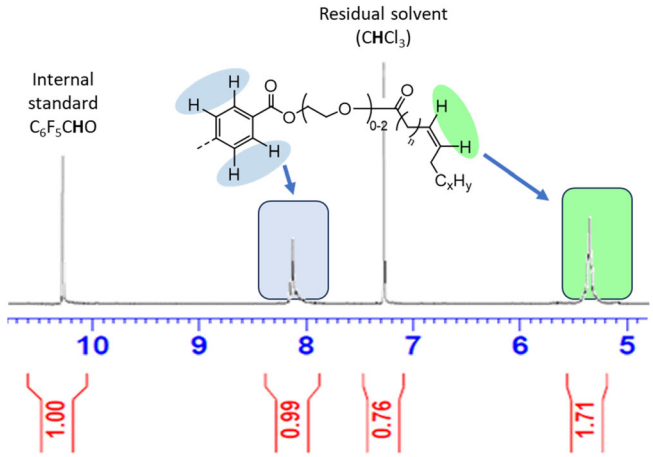

FIGURE 3 Inset of the region of the ^{1}H NMR spectrum used to determine the olefin content of PGB. [Color figure can be viewed at wileyonlinelibrary.com]

(this decomposition event occurs with an onset at ~375°C in PET).

3.2 | Synthesis and chemical characterization of composites

In the final synthetic step to access composites, PGB was reacted with elemental sulfur at 180°C for 24 h with rapid mechanical stirring. The reaction of 80 wt% sulfur and 20 wt% PGB yielded the composite GBS_{80}, while the reaction of 90 wt% sulfur and 10 wt% PGB yielded the composite GBS_{90} (Figure 5). At room temperature (22°C), these composites were black in color and completely remeltable, which allowed them to be poured into silicone molds and reshaped for mechanical analysis. Samples that were remelted several (at least six) times (at 160°C) exhibited properties identical to those made by remelting the initial reaction products, emphasizing the facile thermal recyclability of the materials. Similar recyclability without diminishing mechanical strength has been reported for several other HSMs comprising ≥80 wt % sulfur.[61–64]

SEM with elemental mapping by energy-dispersive x-ray analysis (SEM–EDX) showed that GBS_{80} and GBS_{90} had uniform distributions of carbon, oxygen, and sulfur (Figure 6) and provided evidence of the successful homogenization of the PGB comonomer during the inverse vulcanization reaction.

The FT-IR spectra for GBS_{80} and GBS_{90} composites (Figure S2) showed a reduction in the C—H stretching vibration of the symmetric and asymmetric stretches for CH_2 groups between 2850–2916 cm^{-1} and the disappearance of the C═C stretch, providing evidence for consumption of olefin units during the reaction. Additionally, the emergence of a peak at 664 cm^{-1} in GBS_{80} and GBS_{90} was attributed to the C—S stretch that results from the bonds formed during the inverse vulcanization process.

HSMs like GBS_{80} and GBS_{90} are generally described as composites because some of the sulfur is covalently incorporated into the organic/sulfur-catenate network, while some percentage of free sulfur species is not covalently linked to network organics. The exact nature of this noncovalently incorporated "dark sulfur" is not yet fully known but is being actively studied, notably in insightful studies by Hasell and coworkers.[65,66] A common way to estimate the amount of sulfur covalently incorporated as catenates in the network versus the amount of sulfur entrapped as free sulfur is by extraction of non-covalent sulfur species into a solvent such as CS_2. We thus carried out fractionation studies of GBS_{80} and GBS_{90} by fractionating each into CS_2-souble and -insoluble fractions followed by elemental analysis. This

TABLE 1 Thermal and morphological properties of GBS_x composites with comparison to elemental sulfur and other high sulfur content materials.

Materials	T_d[a]/°C	T_m[b]/°C	$T_{g,DSC}$[c]/°C	Cold crystallization peaks/°C	ΔH_m J/g	ΔH_{cc} J/g	$\%_{xtal}$[d]	Percent insoluble fraction[e]
GBS_{80}	216	117.3	NA	−58.8, 38.8	24.1	2.2, 2.7	43	70
GBS_{90}	217	117.0	NA	−58.8, 37.8	33.4	1.5, 5.3	59	85
mPES	215	116.8	−36.0	3.7	33.6	18.2	33	80
S_8	229	118.5	NA	NA[b]	44.8	NA	100	NA

[a]The temperature at which the 5% mass loss was observed.
[b]The temperature at the peak maximum of the endothermic melting from the third heating cycle.
[c]Glass transition temperature.
[d]Percent crystallinity: the reduction of percent crystallinity of each sample was calculated with respect to sulfur (normalized to 100%).
[e]Percent of nonextractable sulfur in each sample after CS_2 extractions.

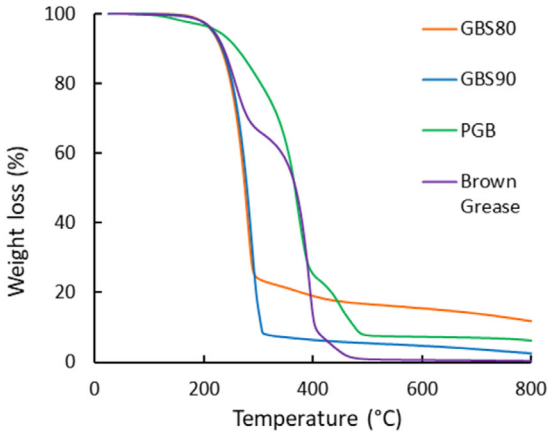

FIGURE 4 Thermogravimetric analysis traces for GBS_{80}, GBS_{90}, brown grease, and PGB. [Color figure can be viewed at wileyonlinelibrary.com]

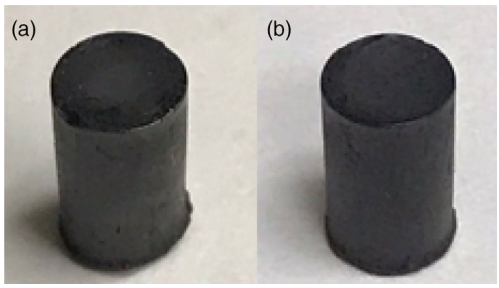

FIGURE 5 Samples of GBS_{80} (a) and GBS_{90} (b) shaped for compressive strength testing. [Color figure can be viewed at wileyonlinelibrary.com]

fractionation revealed that 70% and 85% of sulfur was covalently incorporated into GBS_{80} and GBS_{90}, respectively (Table 1) and that the extractable fraction was >98% sulfur in all cases. Having established the amount of sulfur incorporated into the crosslinked network of the composites via covalent linkages, the average length of the oligosulfur catenates linked to the organic units (knows as sulfur rank) was calculated (Equation S1). For GBS_{90} the sulfur rank was found to be 206. This compares well to other HSMs prepared by the reaction of 90 wt% sulfur and 10 wt% unmodified peanut shells (composite PS_{90}), which had a sulfur rank of 257. In the case of GBS_{80}, the sulfur rank was 60, a value comparable to that in composite LS_{80} (made by reacting allyl lignin with 80 wt% S, sulfur rank = 48), $SunBG_{90}$ (a composite made by combining sunflower oil, brown grease and sulfur in a 1:1:18 mass ratio, with a sulfur rank of 54), and the aforementioned mPES made from waste PET, which had a sulfur rank of 62.

3.3 | Thermal, morphological, and mechanical properties of composites

Thermogravimetric analysis revealed T_d values of 216–217°C for GBS_{80} and GBS_{90}, respectively (Figure 4). This major thermal decomposition event is ubiquitous in HSMs comprising 80–90 wt% S (mPES, e.g., has a T_d of 215°C) and is generally attributed to the sublimation loss of elemental sulfur from the material.

DSC (Figure 7) was employed to investigate the thermal transitions in the composites. GBS_{80} and GBS_{90} exhibited endothermic features at around 105°C attributed to the $\alpha\text{-}S_{(s)} \rightarrow \beta\text{-}S_{(s)}$ phase transition. They also exhibited the typical sulfur melting peak at 117°C, but no apparent T_g was observed in any of the composites over the temperature range investigated (−60 to 140°C). Cold crystallization peaks between −58 and 38°C were present in GBS_{80} and GBS_{90}. These cold crystallization peaks can be attributed to the partial organization of the sulfur catenates chains present in the highly crosslinked composites (Table 1).

The change in crystallinity for GBS_{80} and GBS_{90} relative to crystalline orthorhombic sulfur was calculated from the integration of melting and cold crystallization

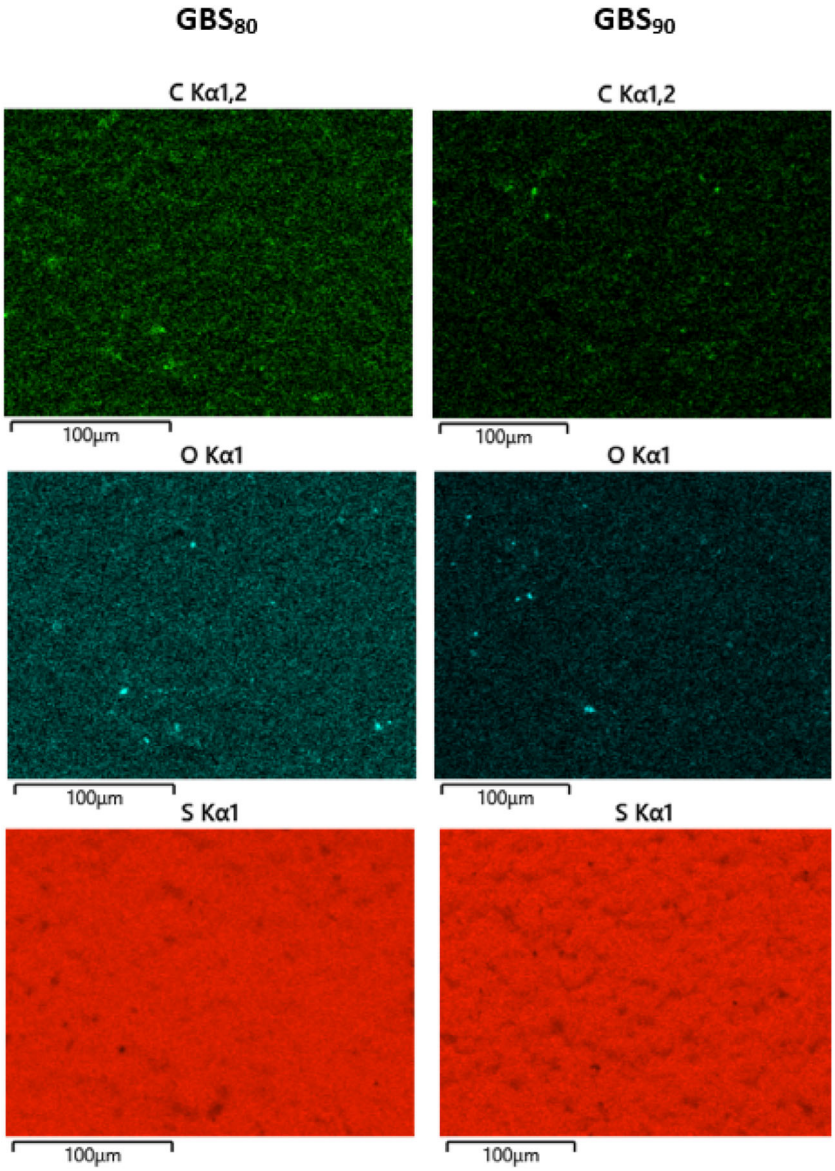

FIGURE 6 Surface analysis of the composites by energy-dispersive x-ray revealed uniform distributions of carbon, oxygen, and sulfur for GBS_{80} (left) and GBS_{90} (right). [Color figure can be viewed at wileyonlinelibrary.com]

enthalpies observed in the DSC thermograms (Table 1). From these integrations, we concluded that GBS_{80} and GBS_{90} composites exhibited percent crystallinities of 43% and 59%, respectively, somewhat higher than the 33% observed in mPES.

To assess whether composites made by this route using waste products could yield materials having excellent mechanical properties comparable to mPES, which contains an expensive and less sustainably sourced olefin, the GBS_x composites were fabricated into shapes appropriate for flexural and compressional strength testing by melting the material at 160°C, pouring the molten solution into a silicon mold, and allowing it to cool to room temperature. This method proved convenient to form requisite cylinders and rectangular prisms appropriate for compressional or flexural strength testing, respectively. All the mechanical test samples were allowed to stand at room temperature for 4 days prior to mechanical testing to allow for direct comparison of the mechanical properties of other HSMs previously reported by our group.[67–71]

Mechanical test stand analysis was used to measure the compressive strengths of the composites (Figure 8a and Table 2; stress–strain plots are provided in Figure S3). The compressive strength of GBS_{80} was 27.5 ± 2.6 MPa, representing 162% of the compressive strength for ordinary Portland cement (OPC) required for building foundations, suggesting that these new composites could serve as OPC replacements. Composite GBS_{90} also exhibited a high compressive strength of 19.2 ± 0.8 MPa, which represents 113% of the compressive strength of OPC. The higher compressive strength of GBS_{80} versus that of GBS_{90} is attributed to the higher organic content present in GBS_{80} that allows for more crosslinking sites during inverse vulcanization.

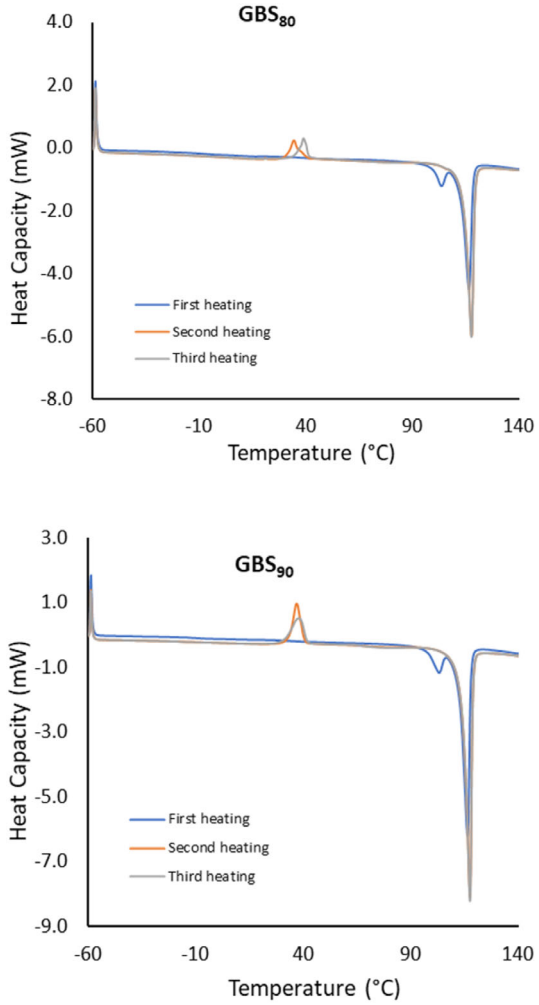

FIGURE 7 Differential scanning calorimetry traces for GBS_{80} and GBS_{90}. Endothermic features are down in these thermograms. [Color figure can be viewed at wileyonlinelibrary.com]

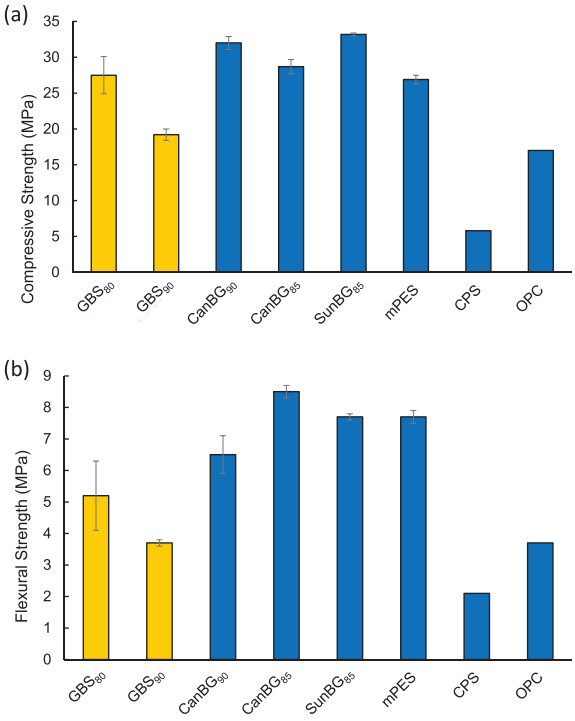

FIGURE 8 Compressive strength (a) and flexural strength (b) for composites GBS_x compared to other high sulfur content materials and ordinary Portland cement (OPC). [Color figure can be viewed at wileyonlinelibrary.com]

GBS_x composites are primarily constituted of aromatic and fatty acid components, so a comparison of their properties to other vulcanized composites in which major components are glycolyzed-PET and/or fatty acid derivatives is most pertinent. Composite mPES, for example, had a compressive strength of 26.9 ± 0.6 MPa, comparable to that of composites GBS_x. Similarly, $CanBG_{90}$ (prepared by reaction of 90 wt% sulfur, 5 wt% brown grease, and 5 wt% canola oil) had a compressive strength of 32.0 ± 0.9 MPa, while $CanBG_{85}$ (prepared by reaction of 5 wt% sulfur, 10 wt% brown grease, and 5 wt% canola oil) and $SunBG_{85}$ (prepared by reaction of 85 wt% sulfur, 10 wt% brown grease, and 5 wt% sunflower oil) had compressive strengths of 28.7 ± 1.0 MPa and 33.2 ± 0.2 MPa, respectively. In another report, composite CPS was synthesized by transesterification of PET with citronellol followed by inverse vulcanization with 90 wt% sulfur.[72] The vulcanization of terpenoid-derived olefins led to a significantly lower compressive strength (5.8 MPa) than was observed for any of the reported materials employing fatty acid chain derived olefins. This observation is consistent with recent mechanistic insight on inverse vulcanization[18] revealing that olefins bearing tertiary carbons (i.e., those in CPS but not in GBS_x) are prone to a higher percentage of linear polymerization and fewer crosslinks, and thus lower anticipated compressive strength.

The flexural strengths/moduli of GBS_{80} and GBS_{90} were also assessed at room temperature in single cantilever mode (Figure 8b and Table 2; stress–strain plots are provided in Figure S4). As observed in the compressive strength trend, GBS_{80} exhibited higher flexural strength/modulus (5.2/210 MPa) than GBS_{90} (3.7/140 MPa). Other HSMs such as $CanBG_{90}$, $CanBG_{85}$, $SunBG_{90}$, $SunBG_{85}$, and mPES had somewhat higher flexural strengths of 6.5–8.5 MPa and moduli of 320–870 MPa. The higher flexural strengths/moduli of these composites can be attributed to the higher olefin content present in brown grease (3.24 mmol g^{-1}) used to prepare $CanBG_{90}$, $CanBG_{85}$, $SunBG_{90}$, and $SunBG_{85}$ than in PGB (1.13 mmol g^{-1}). Similar trends in mechanical strength as a function of olefin content in the monomer feed was observed when various plant oils were reacted with 90 wt % S to form composites.[73] Consistent with the trend observed for compressive strength, terpenoid-bearing

TABLE 2 Physical properties of GBS_x composites with comparison to other high sulfur content materials.

Materials	Compressive strength (MPa)	Flexural strength/ modulus (MPa)	Compressive strength (% of OPC)
GBS_{80}	27.5 ± 2.6	5.2/210	162
GBS_{90}	19.2 ± 0.8	3.7/140	113
$CanBG_{90}$	32.0 ± 0.9	6.5/420	190
$CanBG_{85}$	28.7 ± 1.0	8.5/700	170
$SunBG_{85}$	33.2 ± 0.2	7.7/560	200
mPES	26.9 ± 0.6	7.7/320	158
Portland cement	17.0	3.7/580	100

Abbreviation: OPC, ordinary Portland cement.

composite CPS also has considerably lower flexural strength (2.1 MPa) than the fatty acid chain-bearing materials.[72]

4 | CONCLUSIONS

The route described herein utilizes post-consumer PET, sustainably producible glycols, agricultural by-product brown grease, and energy sector by-product sulfur as chemical reactants to produce high compressive strength composites. Composites GBS_{80} and GBS_{90} both exhibit compressive strengths higher than that of OPC, the most common structural building material currently in use. The current route also represents a significantly more affordable way to access composites over another route we recently reported for the conversion of waste PET to composite mPES, while retaining similar mechanical properties of the end product. The current route thus holds promise as a way to remove waste plastic from the environment while simultaneously replacing less sustainably sourced cement products.

AUTHOR CONTRIBUTIONS

Rhett C. Smith: Funding acquisition (lead); methodology (lead); resources (lead); supervision (lead); writing – review and editing (lead). **Claudia V. Lopez:** Data curation (lead); formal analysis (lead); investigation (lead); validation (lead); writing – original draft (lead).

ACKNOWLEDGMENTS

This research was funded by The National Science Foundation grant number CHE-2203669 and a seed grant from the Animal Coproducts Research and Education Center.

CONFLICT OF INTEREST STATEMENT

The authors declare no conflicts of interest.

DATA AVAILABILITY STATEMENT

Data are available in the Supporting Information file or upon request from the corresponding author.

ORCID

Rhett C. Smith https://orcid.org/0000-0001-6087-8032

REFERENCES

[1] K. L. Scrivener, V. M. John, E. M. Gartner, *Cem. Concr. Res.* **2018**, *114*, 2.
[2] A. Gandini, T. M. Lacerda, A. J. F. Carvalho, E. Trovatti, *Chem. Rev.* **2016**, *116*, 1637.
[3] M. A. R. Meier, J. O. Metzger, U. S. Schubert, *Chem. Soc. Rev.* **2007**, *36*, 1788.
[4] F. Della Monica, A. W. Kleij, *Polym. Chem.* **2020**, *11*, 5109.
[5] P. A. Wilbon, F. Chu, C. Tang, *Macromol. Rapid Commun.* **2013**, *34*, 8.
[6] R. L. Desjardins, D. E. Worth, X. P. Vergé, D. Maxime, J. Dyer, D. Cerkowniak, *Sustainability* **2012**, *4*, 3279.
[7] T. Mekonnen, P. Mussone, D. Bressler, *Crit. Rev. Biotechnol.* **2016**, *36*, 120.
[8] M. J. K. Bashir, L. P. Wong, D. S. Hilaire, J. Kim, O. Salako, M. J. Jean, R. Adeyemi, S. James, T. Foster, L. M. Pratt, *J. Environ. Chem. Eng.* **2020**, *8*, 103848.
[9] M. Kolet, D. Zerbib, F. Nakonechny, M. Nisnevitch, *Catalysts* **2020**, *10*, 1189.
[10] C. Pastore, A. Lopez, G. Mascolo, *Bioresour. Technol.* **2014**, *155*, 91.
[11] Y.-L. Sim, N. Meyappan, N. S. Yen, S. Kamala a/p Subramaniam, C. H. Khoo, W. L. Cheah, D. St. Hilaire, T. Pinnock, B. Bacolod, Z. B. Cai, D. Gurung, R. Hasnat, J. Strothers, C. T. Remy, P. K. Gentles, S. Groveman, M. Vittadello, J. Kim, L. M. Pratt, *Fuel* **2017**, *207*, 274.
[12] J. Strothers, R. B. Matthews, A. Toney, M. R. Cobham, S. Cox, W. Ford, S. Joseph, W. Joyette, S. Khadka, S. Pinnock, M. Burns, M. Noel, M. G. Tamang, D. Saint Hilaire, J.-H. Kim, L. M. Pratt, *Fuel* **2019**, *239*, 573.
[13] M. J. H. Worthington, C. J. Shearer, L. J. Esdaile, J. A. Campbell, C. T. Gibson, S. K. Legg, Y. Yin, N. A. Lundquist, J. R. Gascooke, I. S. Albuquerque, J. G. Shapter, G. G. Andersson, D. A. Lewis, G. J. L. Bernardes, J. M. Chalker, *Adv. Sust. Syst.* **2018**, *2*, 1800024.

[14] M. J. H. Worthington, R. L. Kucera, I. S. Albuquerque, C. T. Gibson, A. Sibley, A. D. Slattery, J. A. Campbell, S. F. K. Alboaiji, K. A. Muller, J. Young, N. Adamson, J. R. Gascooke, D. Jampaiah, Y. M. Sabri, S. K. Bhargava, S. J. Ippolito, D. A. Lewis, J. S. Quinton, A. V. Ellis, A. Johs, G. J. L. Bernardes, J. M. Chalker, *Chem. – Eur. J.* **2017**, *23*, 16219.

[15] N. A. Lundquist, M. J. H. Worthington, N. Adamson, C. T. Gibson, M. R. Johnston, A. V. Ellis, J. M. Chalker, *RSC Adv.* **2018**, *8*, 1232.

[16] C. V. Lopez, A. D. Smith, R. C. Smith, *RSC Adv.* **2022**, *12*, 1535.

[17] W. J. Chung, J. J. Griebel, E. T. Kim, H. Yoon, A. G. Simmonds, H. J. Ji, P. T. Dirlam, R. S. Glass, J. J. Wie, N. A. Nguyen, B. W. Guralnick, J. Park, A. Somogyi, P. Theato, M. E. Mackay, Y.-E. Sung, K. Char, J. Pyun, *Nat. Chem.* **2013**, *5*, 518.

[18] J. Bao, K. P. Martin, E. Cho, K.-S. Kang, R. S. Glass, V. Coropceanu, J.-L. Bredas, W. O. N. Parker Jr., J. T. Njardarson, J. Pyun, *J. Am. Chem. Soc.* **2023**, *145*, 12386.

[19] A. E. Davis, K. B. Sayer, C. L. Jenkins, *Polym. Chem.* **2022**, *13*, 4634.

[20] M. L. Eder, C. B. Call, C. L. Jenkins, *ACS Appl. Polym. Mater.* **2022**, *4*, 1110.

[21] J. A. Smith, S. J. Green, S. Petcher, D. J. Parker, B. Zhang, M. J. H. Worthington, X. Wu, C. A. Kelly, T. Baker, C. T. Gibson, J. A. Campbell, D. A. Lewis, M. J. Jenkins, H. Willcock, J. M. Chalker, T. Hasell, *Chem. Eur. J.* **2019**, *25*, 10433.

[22] C. R. Westerman, C. L. Jenkins, *Macromolecules* **2018**, *51*, 7233.

[23] P. Yan, W. Zhao, S. J. Tonkin, J. M. Chalker, T. L. Schiller, T. Hasell, *Chem. Mater.* **2022**, *34*, 1167.

[24] P. Yan, W. Zhao, F. McBride, D. Cai, J. Dale, V. Hanna, T. Hasell, *Nat. Commun.* **2022**, *13*, 4824.

[25] J. Jia, J. Liu, Z.-Q. Wang, T. Liu, P. Yan, X.-Q. Gong, C. Zhao, L. Chen, C. Miao, W. Zhao, S. Cai, X.-C. Wang, A. I. Cooper, X. Wu, T. Hasell, Z.-J. Quan, *Nat. Chem.* **2022**, *14*, 1249.

[26] M. Mann, X. Luo, A. D. Tikoalu, C. T. Gibson, Y. Yin, R. Al-Attabi, G. G. Andersson, C. L. Raston, L. C. Henderson, A. Pring, T. Hasell, J. M. Chalker, *Chem. Commun.* **2021**, *57*, 6296.

[27] P. Yan, W. Zhao, B. Zhang, L. Jiang, S. Petcher, J. A. Smith, D. J. Parker, A. I. Cooper, J. Lei, T. Hasell, *Angew. Chem., Int. Ed.* **2020**, *59*, 13371.

[28] S. J. Tonkin, C. T. Gibson, J. A. Campbell, D. A. Lewis, A. Karton, T. Hasell, J. M. Chalker, *Chem. Sci.* **2020**, *11*, 5537.

[29] T. Hasell, P. Yan, W. Zhao, B. Zhang, S. Petcher, A. Smith Jessica, J. Parker Douglas, I. Cooper Andrew, L. Jiang, J. Lei, *Angew. Chem. Int. Ed. in English* **2020**, *59*, 2.

[30] F. G. Mueller, L. S. Lisboa, J. M. Chalker, *Adv. Sustainable Syst.* **2023**, *7*, 2300010.

[31] A. Gupta, M. J. H. Worthington, H. D. Patel, M. R. Johnston, M. Puri, J. M. Chalker, *ACS ACS Sustainable Chem. Eng.* **2022**, *10*, 9022.

[32] N. A. Lundquist, A. D. Tikoalu, M. J. H. Worthington, R. Shapter, S. J. Tonkin, F. Stojcevski, M. Mann, C. T. Gibson, J. R. Gascooke, A. Karton, L. C. Henderson, L. J. Esdaile, J. M. Chalker, *Chem. Eur. J.* **2020**, *26*, 10035.

[33] J. M. Chalker, M. J. H. Worthington, N. A. Lundquist, L. J. Esdaile, *Top. Curr. Chem.* **2019**, *377*, 1.

[34] A. D. Smith, R. C. Smith, A. G. Tennyson, *Sustainable Chem. Pharm.* **2020**, *16*, 100249.

[35] X. Wu, J. A. Smith, S. Petcher, B. Zhang, D. J. Parker, J. M. Griffin, T. Hasell, *Nat. Commun.* **2019**, *10*, 10035.

[36] B. Zhang, S. Petcher, T. Hasell, *Chem. Commun.* **2019**, *55*, 10681.

[37] R. Westerman Clayton, M. Walker Princess, L. J. Courtney, *J. Visualized Exp.* **2019**, *147*, e59620.

[38] S. Sahu, B. Lochab, *ACS Sustainable Chem. Eng.* **2022**, *10*, 12355.

[39] M. Mann, P. J. Pauling, S. J. Tonkin, J. A. Campbell, J. M. Chalker, *Macromol. Chem. Phys.* **2022**, *223*, 2100333.

[40] J. J. Griebel, S. Namnabat, E. T. Kim, R. Himmelhuber, D. H. Moronta, W. J. Chung, A. G. Simmonds, K.-J. Kim, J. van der Laan, N. A. Nguyen, E. L. Dereniak, M. E. MacKay, K. Char, R. S. Glass, R. A. Norwood, J. Pyun, *Adv. Mater.* **2014**, *26*, 3014.

[41] H.-K. Lin, Y.-S. Lai, Y.-L. Liu, *ACS Sustainable Chem. Eng.* **2019**, *7*, 4515.

[42] A. M. Abraham, S. V. Kumar, S. M. Alhassan, *Chem. Eng. J.* **2018**, *332*, 1.

[43] D. J. Parker, H. A. Jones, S. Petcher, L. Cervini, J. M. Griffin, R. Akhtar, T. Hasell, *J. Mater. Chem. A* **2017**, *5*, 11682.

[44] S. Akay, B. Kayan, D. Kalderis, M. Arslan, Y. Yagci, B. Kiskan, *J. Appl. Polym. Sci.* **2017**, *134*, 45306.

[45] T. Hasell, D. J. Parker, H. A. Jones, T. McAllister, S. M. Howdle, *Chem. Commun.* **2016**, *52*, 5383.

[46] Z. Chen, J. Droste, G. Zhai, J. Zhu, J. Yang, M. R. Hansen, X. Zhuang, *Chem. Commun.* **2019**, *55*, 9047.

[47] F. Zhao, Y. Li, W. Feng, *Small Methods* **2018**, *2*, 1.

[48] D. T. Nguyen, A. Hoefling, M. Yee, G. T. H. Nguyen, P. Theato, Y. J. Lee, S.-W. Song, *ChemSusChem* **2019**, *12*, 480.

[49] A. Hoefling, D. T. Nguyen, P. Partovi-Azar, D. Sebastiani, P. Theato, S.-W. Song, Y. J. Lee, *Chem. Mater.* **2018**, *30*, 2915.

[50] A. Hoefling, D. T. Nguyen, Y. J. Lee, S.-W. Song, P. Theato, *Mater. Chem. Front.* **2017**, *1*, 1818.

[51] A. Hoefling, Y. J. Lee, P. Theato, *Macromol. Chem. Phys.* **2017**, *218*, 1600303.

[52] P. T. Dirlam, A. G. Simmonds, T. S. Kleine, N. A. Nguyen, L. E. Anderson, A. O. Klever, A. Florian, P. J. Costanzo, P. Theato, M. E. Mackay, R. S. Glass, K. Char, J. Pyun, *RSC Adv.* **2015**, *5*, 24718.

[53] G. Hernandez, N. Casado, A. M. Zamarayeva, J. K. Duey, M. Armand, A. C. Arias, D. Mecerreyes, *ACS Appl. Energy Mater.* **2018**, *1*, 7199.

[54] I. Gomez, O. Leonet, J. Alberto Blazquez, H.-J. Grande, D. Mecerreyes, *ACS Macro Lett.* **2018**, *7*, 419.

[55] I. Gomez, O. Leonet, J. A. Blazquez, D. Mecerreyes, *ChemSusChem* **2016**, *9*, 3419.

[56] S. F. Valle, A. S. Giroto, R. Klaic, G. G. F. Guimaraes, C. Ribeiro, *Polym. Degrad. Stab.* **2019**, *162*, 102.

[57] M. Mann, J. E. Kruger, F. Andari, J. McErlean, J. R. Gascooke, J. A. Smith, M. J. H. Worthington, C. C. C. McKinley, J. A. Campbell, D. A. Lewis, T. Hasell, M. V. Perkins, J. M. Chalker, *Org. Biomol. Chem.* **2019**, *17*, 1929.

[58] T. Thiounn, M. S. Karunarathna, M. K. Lauer, A. G. Tennyson, R. C. Smith, *RSC Sustainable* **2023**, *1*, 535.

[59] C. P. Maladeniya, A. G. Tennyson, R. C. Smith, *J. Polym. Sci.* **2023**, *61*, 787.

[60] C. V. Lopez, R. C. Smith, *Mater. Adv.* **2023**, *4*, 2785.
[61] M. K. Lauer, M. S. Karunarathna, A. G. Tennyson, R. C. Smith, *Mater. Adv.* **2020**, *1*, 2271.
[62] P. Y. Sauceda-Oloño, A. C. Borbon-Almada, M. Gaxiola, A. D. Smith, A. G. Tennyson, R. C. Smith, *J. Compos. Sci.* **2023**, *7*, 248.
[63] A. D. Smith, T. Thiounn, E. W. Lyles, E. K. Kibler, R. C. Smith, A. G. Tennyson, *J. Poly. Sci. A* **2019**, *57*, 1704.
[64] M. K. Lauer, M. S. Karunarathna, A. G. Tennyson, R. C. Smith, *Mater. Adv.* **2020**, *1*, 590.
[65] J. J. Dale, S. Petcher, T. Hasell, *ACS Appl. Polym. Mater.* **2022**, *4*, 3169.
[66] J. J. Dale, J. Stanley, R. A. Dop, G. Chronowska-Bojczuk, A. J. Fielding, D. R. Neill, T. Hasell, *Eur. Polym. J.* **2023**, *195*, 112198.
[67] M. K. Lauer, A. G. Tennyson, R. C. Smith, *ACS Appl. Polym. Mater.* **2020**, *2*, 3761.
[68] K. A. Tisdale, C. P. Maladeniya, C. V. Lopez, A. G. Tennyson, R. C. Smith, *J. Compos. Sci.* **2023**, *7*, 35.
[69] M. J. Graham, C. V. Lopez, C. P. Maladeniya, A. G. Tennyson, R. C. Smith, *J. Appl. Polym. Sci.* **2023**, *140*, e53684.
[70] C. P. Maladeniya, R. C. Smith, *J. Compos. Sci.* **2021**, *5*, 257.
[71] C. P. Maladeniya, M. S. Karunarathna, M. K. Lauer, C. V. Lopez, T. Thiounn, R. C. Smith, *Mater. Adv.* **2020**, *1*, 1665.
[72] K. M. Derr, C. V. Lopez, C. P. Maladeniya, A. G. Tennyson, R. C. Smith, *J. Appl. Polym. Sci.* **2023**. Epub ahead of print. https://doi.org/10.1002/pol.20230503
[73] C. V. Lopez, M. S. Karunarathna, M. K. Lauer, C. P. Maladeniya, T. Thiounn, E. D. Ackley, R. C. Smith, *J. Poly. Sci.* **2020**, *58*, 2259.

SUPPORTING INFORMATION

Additional supporting information can be found online in the Supporting Information section at the end of this article.

How to cite this article: C. V. Lopez, R. C. Smith, *J. Appl. Polym. Sci.* **2023**, e54828. https://doi.org/10.1002/app.54828